

A UNIFIED EQUILIBRATED FLUX RECOVERY FRAMEWORK WITH ROBUST A POSTERIORI ERROR ESTIMATION

CUIYU HE*

Abstract. We introduce the Equilibrated Averaging Residual Method (EARM), a unified equilibrated flux-recovery framework for elliptic interface problems that applies to a broad class of finite element discretizations. The method is applicable in both two and three dimensions and for arbitrary polynomial orders, and it enables the construction of computationally efficient recovered fluxes. We develop EARM for both discontinuous Galerkin (DG) and conforming finite element discretizations. For DG methods, EARM can be applied directly and yields an explicit recovered flux that coincides with state-of-the-art conservative flux reconstructions.

For conforming discretizations, we further propose the Orthogonal Null-space-Eliminated EARM (ON-EARM), which ensures uniqueness by restricting the correction flux to the orthogonal complement of the divergence-free null space. We prove local conservation and establish a robust a posteriori error estimator for the recovered flux in two dimensions, with robustness measured with respect to jumps in the diffusion coefficient. Numerical results in two and three dimensions confirm the theoretical findings.

Key words. EARM, ON-EARM, Adaptive Mesh Refinement; Equilibrated Flux Recovery; a posteriori Error Estimation.

AMS subject classifications. 65N30 65N50

1. Introduction. An accurate and locally conservative recovered flux (also referred to as an equilibrated flux) for finite element (FE) solutions plays a central role in many applications, including a posteriori error estimation [1, 11, 33, 9, 24, 13, 16], a key component of adaptive mesh refinement, compatible transport in heterogeneous media [29], and velocity reconstruction in porous media [22, 34, 5, 19], among others.

In this work, we focus on equilibrated flux recovery and its associated a posteriori error estimation for elliptic interface problems, allowing for large jumps in the diffusion coefficient. Equilibrated estimators have attracted significant attention due to their guaranteed reliability for the conforming error of the finite element solution: specifically, the reliability constant of an equilibrated a posteriori error estimator equals one for the conforming error. This property makes such estimators particularly well-suited for discretization error control on both coarse and fine meshes.

The mathematical foundation of equilibrated a posteriori error estimation for conforming finite element approximations is the Prager–Synge identity [31], which is valid for $H^1(\Omega)$ -conforming approximations. A generalized Prager–Synge identity for piecewise $H^1(\Omega)$ (possibly discontinuous) finite element approximations in both two and three dimensions was established in [16]. There, the error is decomposed into conforming and nonconforming components, and the conforming part is guaranteed to be bounded by an equilibrated error estimator, given by the energy norm of the difference between the numerical flux and a recovered equilibrated flux.

In this paper, we introduce a unified equilibrated flux-recovery framework for a broad class of finite element methods. The method applies in both two and three dimensions and for arbitrary polynomial orders. Due to space limitations, we restrict the development to conforming and discontinuous Galerkin (DG) methods in two and

*Department of Mathematics, University of Georgia, Athens, GA (cuiyu.he@uga.edu).

three dimensions. In the DG case, the recovered flux coincides with state-of-the-art locally conservative flux reconstructions.

In EARM, the recovered flux is constructed as the sum of two components: an averaged numerical flux obtained explicitly from the discrete finite element solution, and a correction flux. The correction flux is computed by solving a variational problem whose right-hand side is given by a residual operator associated with the averaged numerical flux. For this reason, we call the approach the *Equilibrated Averaging Residual Method* (EARM), to distinguish it from the classical equilibrated residual method of [3].

It is important to note that the variational problem underlying EARM for solving the correction flux admits infinitely many solutions, since its null space is precisely the space of divergence-free fluxes. Our goal is to identify and solve one flux solution that is equilibrated and sufficiently accurate to guarantee the robust local efficiency in the a posteriori error analysis, while also being computationally efficient to compute.

Discontinuous Galerkin (DG) methods are well known for inherently ensuring local equilibria. We refer to [1, 23] and references therein for earlier works on explicit conservative flux reconstructions of linear and higher-order DG elements in elliptic problems. Notably, one obvious solution to the EARM for DG solutions naturally coincides with the results in [1] and [23] for linear and arbitrary-order DG finite element solutions.

Many researchers have studied conservative flux recovery methods for conforming finite element methods (FEM); see, for example, [25, 20, 28, 21, 3, 2, 26, 32, 8, 11, 10, 33, 17, 6, 29, 13, 24]. Partition of unity (POU) techniques are commonly employed for localization, particularly in the absence of explicit construction techniques.

Using a POU argument, Ladevèze and Leguillon [25] initiated a local procedure that reduces the construction of an equilibrated flux to vertex patch-based local problems. For continuous linear finite element approximations of the Poisson equation in two dimensions, an equilibrated flux in the lowest-order Raviart–Thomas space was explicitly constructed in [8, 11]. Without introducing a constraint minimization step (see [17]), however, this explicit construction does not yield a robust a posteriori error estimator with respect to jumps in the diffusion coefficient. The required constraint minimization problem on each vertex patch can be addressed by first computing an equilibrated flux and then applying a divergence-free correction. For recent developments along these lines, we refer to [13] and the references therein.

In [24], a unified approach, also based on POU techniques, was developed. This method requires solving local mixed problems on vertex patches associated with each mesh vertex. In contrast, the approaches in [26, 29] compute a conservative flux by solving a global problem posed on an enriched piecewise-constant DG space.

The equilibrated residual method of [3] (Chapter 6.4) also constructs a conservative flux for conforming FEM via a partition-of-unity (POU) localization. Rather than solving directly for the flux, the method first computes its moments, which naturally localizes the construction to star-patch regions. However, the local star-patch problem associated with each interior vertex (and with certain boundary vertices) has a one-dimensional kernel. To remove this indeterminacy, an additional constraint is imposed, and the resulting constrained local problem is typically solved via a Lagrange-multiplier formulation. Finally, the global flux is assembled from the computed moments.

In principle, POU localization can be applied uniformly to a wide range of finite element methods, since it does not rely on any special structure of the underlying basis functions. In practice, however, it is mainly used for continuous Galerkin (CG)

discretizations, because simpler recovery procedures are available for discontinuous Galerkin (DG) methods. Accordingly, POU-based constructions are often relatively involved, as they require the solution of star-patch local problems that are either constrained [17] or posed in a mixed formulation [24].

For localization approaches beyond POU-based methods, we refer to [6], which studies two-dimensional Poisson problems. There, a unified mixed formulation is proposed for continuous, nonconforming, and discontinuous Galerkin methods in two dimensions. By replacing the exact facet integrals with an inexact Gauss–Lobatto quadrature, the construction can be localized, yielding conservative fluxes for a range of FEM discretizations. Extending this approach to three dimensions in the conforming case is, however, not straightforward: the constraints imposed on the skeleton space in two dimensions do not admit an obvious analogue in three dimensions, and an appropriate Gauss–Lobatto-type quadrature rule is not available on tetrahedral meshes.

In this paper, we propose the Orthogonal Null-space–Eliminated Equilibrated Averaging Residual Method (ON-EARM), for which no partition-of-unity (POU) localization is required. To ensure uniqueness, we eliminate the null space by restricting the correction flux to the orthogonal complement of the divergence-free null space. We show that the space generated by facet jumps of DG functions is contained in this orthogonal complement, which yields a well-posed variational formulation with a unique solution.

The resulting space-restricted variational problem leads to a global linear system whose unknowns are restricted to facet degrees of freedom; consequently, its dimension is substantially smaller than that of the linear system arising from the original PDE discretization. In the lowest-order (0th-order) DG case, the resulting flux coincides with the constructions in [26, 29].

We note that, for linear and higher-order elements in two dimensions, the global variational formulation can be localized following [6] by replacing the exact facet integrals with an inexact Gauss–Lobatto quadrature. In this case, the resulting recovered flux coincides with that of [6] and can be computed fully explicitly, as demonstrated in [18].

Unlike in two dimensions, where Gauss–Lobatto quadrature yields a fully localized construction, no analogous Gauss–Lobatto-type rule is available on tetrahedral meshes in three dimensions. While tetrahedral quadrature rules with vertex evaluations exist, their low polynomial exactness makes them unsuitable for comparable localization and accuracy. This limitation is specific to tetrahedra: on hexahedral meshes, tensor-product Gauss–Lobatto rules retain vertex evaluations and high exactness, enabling full localization. We do not analyze these localized three-dimensional variants here; the two-dimensional case is covered in [6], and a corresponding hexahedral analysis can likely be developed along similar lines.

Equilibrated a posteriori error estimators are distinguished by the fact that their reliability constant is exactly equal to one for the conforming error. In this work, we preserve this property within the proposed EARM/ON-EARM framework. Moreover, in two dimensions we establish a robust efficiency bound for the error indicators associated with ON-EARM, where robustness means independence with respect to jumps in the diffusion coefficient. Together, these results provide a fully reliable and robust a posteriori error estimation framework suitable for adaptive finite element methods applied to elliptic interface problems.

Numerically, we test the method on a collection of singular benchmark problems that are representative of interface effects and geometric singularities arising in

adaptive mesh refinement procedures.

In two dimensions, we consider the Kellogg interface problem and the L-shaped domain problem, and report results for the polynomial degrees $k = 1, 2, 3$. In three dimensions, we study an L-shaped domain with a vertex singularity, again for $k = 1, 2, 3$. All these examples involve strong solution singularities and are chosen to assess the robustness of the method under challenging conditions. What we observe is optimal, and in some cases even super-convergence behavior, across all test cases.

The remainder of this paper is organized as follows. In [section 2](#), we introduce the model problem and the notations. In [section 3](#) and [section 4](#), we apply EARM to discontinuous Galerkin and conforming discretizations, respectively, and show that the resulting reconstructions recover several existing state-of-the-art locally conservative fluxes. In [section 5](#), we establish the reliability of the associated a posteriori error estimator, while [section 6](#) is devoted to the efficiency analysis, including robustness with respect to coefficient jumps. Finally, numerical results are reported in [section 7](#).

2. Model problem. Let Ω be a bounded polygonal domain in \mathbb{R}^d , $d = 2, 3$, with Lipschitz boundary $\partial\Omega = \bar{\Gamma}_D \cup \bar{\Gamma}_N$, where $\Gamma_D \cap \Gamma_N = \emptyset$. For simplicity, assume that $\text{meas}_{d-1}(\Gamma_D) \neq 0$. Considering the diffusion problem:

$$(2.1) \quad -\nabla \cdot (A\nabla u) = f \quad \text{in } \Omega,$$

with boundary conditions

$$u = 0 \quad \text{on } \Gamma_D \quad \text{and} \quad -A\nabla u \cdot \mathbf{n} = g \quad \text{on } \Gamma_N,$$

where $\nabla \cdot$ and ∇ are the respective divergence and gradient operators; \mathbf{n} is the outward unit vector normal to the boundary; $f \in H^{-1}(\Omega)$ and $g \in H^{-1/2}(\Gamma_N)$ are given scalar-valued functions; and the diffusion coefficient $A(x)$ is symmetric, positive definite, piecewise constant full tensor.

In this paper, we use the standard notations and definitions for the Sobolev spaces. Let

$$H_D^1(\Omega) = \{v \in H^1(\Omega) : v = 0 \text{ on } \Gamma_D\}.$$

Then the corresponding variational problem of (2.1) is to find $u \in H_D^1(\Omega)$ such that

$$(2.2) \quad a(u, v) := (A\nabla u, \nabla v) = (f, v)_\Omega - \langle g, v \rangle_{\Gamma_N}, \quad \forall v \in H_D^1(\Omega),$$

where $(\cdot, \cdot)_\omega$ is the L^2 inner product on the domain ω . The subscript ω is omitted from here to thereafter when $\omega = \Omega$.

2.1. Notations. Let $\mathcal{T}_h = \{K\}$ be a finite element partition of Ω that is regular, and denote by h_K the diameter of the element K . Denote the set of all facets of the triangulation \mathcal{T}_h by

$$\mathcal{E} := \mathcal{E}_I \cup \mathcal{E}_D \cup \mathcal{E}_N,$$

where \mathcal{E}_I is the set of interior element facets, and \mathcal{E}_D and \mathcal{E}_N are the sets of boundary facets belonging to the respective Γ_D and Γ_N . For each $F \in \mathcal{E}$, denote by h_F the length of F and by \mathbf{n}_F a unit vector normal to F . Let K_F^+ and K_F^- be the two elements sharing the common facet $F \in \mathcal{E}_I$ such that the unit outward normal of K_F^- coincides with \mathbf{n}_F . When $F \in \mathcal{E}_D \cup \mathcal{E}_N$, \mathbf{n}_F is the unit outward normal to $\partial\Omega$ and denote by K_F^- the element having the facet F . Note here that the term facet refers to the $d-1$ dimensional entity of the mesh. In 2D, a facet is equivalent to an edge, and in 3D, it is equivalent to a face. We also denote by \mathcal{N} the set of all vertices and by $\mathcal{N}_I \subset \mathcal{N}$ the set of interior vertices.

For each $K \in \mathcal{T}_h$ ($F \in \mathcal{E}$), let $\mathbb{P}_k(K)(\mathbb{P}_k(F))$ denote the space of polynomials of degree at most k on $K(F)$. For each $K \in \mathcal{T}_h$, we define a sign function $\text{sign}_K(F)$ on $\mathcal{E}_K := \{F : F \in \mathcal{E}, \text{ and } F \subset \partial K\}$:

$$\text{sign}_K(F) = \begin{cases} 1 & \text{if } \mathbf{n}_F = \mathbf{n}_K|_F, \\ -1 & \text{if } \mathbf{n}_F = -\mathbf{n}_K|_F. \end{cases}$$

3. The EARM and Its Application to DG FEM. In this section, we introduce the EARM and apply it to the DG finite element method. The resulting equilibrated fluxes for DG solutions recover existing state-of-the-art constructions in certain special cases, while employing modified weights to ensure robustness.

Define

$$DG(\mathcal{T}_h, k) = \{v \in L^2(\Omega) : v|_K \in \mathbb{P}_k(K), \forall K \in \mathcal{T}_h\}.$$

Denote the $H(\text{div}; \Omega)$ conforming Raviart-Thomas (RT) space of order k with respect to \mathcal{T}_h by

$$RT(\mathcal{T}_h, k) = \{\boldsymbol{\tau} \in H(\text{div}; \Omega) : \boldsymbol{\tau}|_K \in RT(K, k), \forall K \in \mathcal{T}_h\},$$

where $RT(K, k) = \mathbb{P}_k(K)^d + \mathbf{x} \mathbb{P}_k(K)$. Also let

$$RT_f(\mathcal{T}_h, k) = \{\boldsymbol{\tau} \in RT(\mathcal{T}_h, k) : \nabla \cdot \boldsymbol{\tau} = f_k \text{ in } \Omega \text{ and } \boldsymbol{\tau} \cdot \mathbf{n}_F = g_{k,F} \text{ on } F \in \mathcal{E}_N\},$$

where f_k is the L^2 projection of f onto $DG(\mathcal{T}_h, k)$ and $g_{k,F}$ is the L^2 projection of $g|_F$ onto $\mathbb{P}_k(F)$.

For each $F \in \mathcal{E}_I$, we define the following weights: $\omega_F^\pm = \frac{\alpha_F^\mp}{\alpha_F^- + \alpha_F^+}$ where $\alpha_F^\pm = \lambda(A|_{K_F^\pm})$ and $\lambda(M)$ is the maximal eigenvalue of the matrix M . We also define the following weighted average and jump operators:

$$\{v\}_w^F = \begin{cases} w_F^+ v_F^+ + w_F^- v_F^-, & F \in \mathcal{E}_I, \\ v, & F \in \mathcal{E}_D \cup \mathcal{E}_N, \end{cases} \quad \{v\}_F^w = \begin{cases} w_F^- v_F^+ + w_F^+ v_F^-, & F \in \mathcal{E}_I, \\ 0, & F \in \mathcal{E}_D \cup \mathcal{E}_N, \end{cases}$$

$$[\![v]\!]_F = \begin{cases} v|_F^- - v|_F^+, & \forall F \in \mathcal{E}_I, \\ v|_F^-, & \forall F \in \mathcal{E}_D \cup \mathcal{E}_N. \end{cases}$$

The weighted average defined above is necessary to ensure the robustness of the error estimation with respect to the jump of A , see [15]. It is easy to show that for any $F \in \mathcal{E}_I$,

$$(3.1) \quad w_F^\pm \sqrt{\alpha_F^\pm} \leq \sqrt{\alpha_{F,\min}}, \quad \frac{\omega_F^+}{\sqrt{\alpha_F^-}} \leq \sqrt{\frac{1}{\alpha_{F,\max}}}, \quad \text{and} \quad \frac{\omega_F^-}{\sqrt{\alpha_F^+}} \leq \sqrt{\frac{1}{\alpha_{F,\max}}},$$

where $\alpha_{F,\min} = \min(\alpha_F^+, \alpha_F^-)$ and $\alpha_{F,\max} = \max(\alpha_F^+, \alpha_F^-)$.

We will also use the following commonly used identity:

$$(3.2) \quad [\![uv]\!]_F = \{v\}_F^w [\![u]\!]_F + \{u\}_w^F [\![v]\!]_F, \quad \forall F \in \mathcal{E}.$$

We first present the DG variational formulation for (2.1): find $u \in V^{1+\epsilon}(\mathcal{T}_h)$ with $\epsilon > 0$ and

$$V^s(\mathcal{T}_h) = \{v \in L^2(\Omega), v|_K \in H^s(K) \text{ and } \nabla \cdot A \nabla v \in L^2(K), \forall K \in \mathcal{T}_h\}$$

such that

$$(3.3) \quad a_{dg}(u, v) = (f, v) - \langle g, v \rangle_{\Gamma_N}, \quad \forall v \in V^{1+\epsilon}(\mathcal{T}_h),$$

where

$$(3.4) \quad \begin{aligned} a_{dg}(u, v) &= (A\nabla_h u, \nabla_h v) + \sum_{F \in \mathcal{E} \setminus \mathcal{E}_N} \int_F \gamma \frac{\alpha_{F,min}}{h_F} \llbracket u \rrbracket \llbracket v \rrbracket ds \\ &\quad - \sum_{F \in \mathcal{E} \setminus \mathcal{E}_N} \int_F \{A\nabla u \cdot \mathbf{n}_F\}_w^F \llbracket v \rrbracket ds + \delta \sum_{F \in \mathcal{E} \setminus \mathcal{E}_N} \int_F \{A\nabla v \cdot \mathbf{n}_F\}_w^F \llbracket u \rrbracket ds. \end{aligned}$$

Here, ∇_h is the discrete gradient operator defined elementwisely, and γ is a positive constant, δ is a constant that takes value 1, 0 or -1 .

The DG solution is to seek $u_k^{dg} \in DG(\mathcal{T}_h, k)$ such that

$$(3.5) \quad a_{dg}(u_k^{dg}, v) = (f, v)_\Omega - \langle g, v \rangle_{\Gamma_N} \quad \forall v \in DG(\mathcal{T}_h, k).$$

Note that the numerical flux, $-A\nabla u_k^{dg}$, does not necessarily belong to the space $H(\text{div}; \Omega)$. In the first step of EARM, we define a functional for any $u_h \in DG(\mathcal{T}_h, k)$:

$$\tilde{\boldsymbol{\sigma}}_s : u_h \in DG(\mathcal{T}_h, k) \rightarrow \tilde{\boldsymbol{\sigma}}_s(u_h) \in RT(\mathcal{T}_h, s), \quad 0 \leq s \leq k,$$

such that

$$(3.6) \quad \int_F \tilde{\boldsymbol{\sigma}}_s(u_h) \cdot \mathbf{n}_F \phi ds = \begin{cases} - \int_F \{A\nabla u_h \cdot \mathbf{n}_F\}_w^F \phi ds & \forall F \in \mathcal{E} \setminus \mathcal{E}_N, \\ \int g \phi ds, & \forall F \in \mathcal{E}_N, \end{cases} \quad \forall \phi \in \mathbb{P}_s(F).$$

and when $s \geq 1$, additionally satisfies that

$$(3.7) \quad (\tilde{\boldsymbol{\sigma}}_s(u_h), \boldsymbol{\psi})_K = -(A\nabla u_h, \boldsymbol{\psi})_K, \quad \forall K \in \mathcal{T}_h, \forall \boldsymbol{\psi} \in \mathbb{P}_{s-1}(K)^d.$$

Since the recovered flux $\tilde{\boldsymbol{\sigma}}_s(u_h)$ uses the averaging flux on the facets, we will refer to this flux as the *averaging numerical flux* of u_h .

For simplicity, we assume that $g|_F = g_{k-1,F}$. Since $\{A\nabla u_k^{cg} \cdot \mathbf{n}_F\}_w^F \in \mathbb{P}_{k-1}(F)$, it is easy to see that when $s \geq k-1$, there holds

$$(3.8) \quad \tilde{\boldsymbol{\sigma}}_s(u_h) \cdot \mathbf{n}_F = \begin{cases} -\{A\nabla u_h \cdot \mathbf{n}_F\}_w^F & \forall F \in \mathcal{E} \setminus \mathcal{E}_N, \\ g, & \forall F \in \mathcal{E}_N. \end{cases}$$

We note that the weighted averaging flux $\tilde{\boldsymbol{\sigma}}_s^{dg} := \tilde{\boldsymbol{\sigma}}_s(u_k^{dg}) \in H(\text{div}; \Omega)$, however, is not necessarily locally conservative.

In the second step of EARM, we aim to find a correction flux $\boldsymbol{\sigma}_s^\Delta \in RT(\mathcal{T}_h, s)$ such that

$$(3.9) \quad \hat{\boldsymbol{\sigma}}_s^{dg} := \tilde{\boldsymbol{\sigma}}_s^{dg} + \boldsymbol{\sigma}_s^\Delta \in RT_f(\mathcal{T}_h, s).$$

Define the *averaging residual operator* for any u_h being a finite element solution:

$$(3.10) \quad r_s(v) = \sum_K r_{s,K}(v), \quad \text{where } r_{s,K}(v) := (f - \nabla \cdot \tilde{\boldsymbol{\sigma}}_s(u_h), v)_K.$$

Our goal is to find $\boldsymbol{\sigma}_s^\Delta \in RT(\mathcal{T}_h, s)$ for u_h such that

$$(3.11) \quad (\nabla \cdot \boldsymbol{\sigma}_s^\Delta, v) = r_s(v) \quad \forall v \in DG(\mathcal{T}_h, s).$$

We now set to find a $\boldsymbol{\sigma}_s^\Delta \in RT(\mathcal{T}_h, s)$ specifically for the DG finite element solution u_k^{dg} . By the integration by parts, the definition of $\tilde{\boldsymbol{\sigma}}_s^{dg}$ and (3.5), for any $v \in \mathbb{P}_s(K)$, there holds

$$(3.12) \quad \begin{aligned} r_s(v) &= (f, v)_K + (\tilde{\boldsymbol{\sigma}}_s^{dg}, \nabla v)_K - \langle \tilde{\boldsymbol{\sigma}}_s^{dg} \cdot \mathbf{n}_K, v \rangle_{\partial K} \\ &= (f, v)_K - (A \nabla u_k^{dg}, \nabla v)_K + \sum_{F \in \mathcal{E}_K \setminus \mathcal{E}_N} \int_F \{A \nabla u_k^{dg} \cdot \mathbf{n}_F\}_w^F \llbracket v \rrbracket ds - \sum_{F \in \mathcal{E}_K \cap \mathcal{E}_N} \langle g, v \rangle_F \\ &= \sum_{F \in \mathcal{E}_K \setminus \mathcal{E}_N} \int_F \gamma \frac{\alpha_{F, \min}}{h_F} \llbracket u_k^{dg} \rrbracket \llbracket v \rrbracket ds + \delta \sum_{F \in \mathcal{E}_K \setminus \mathcal{E}_N} \int_F \{A \nabla v \cdot \mathbf{n}_F\}_w^F \llbracket u_k^{dg} \rrbracket ds. \end{aligned}$$

On the other side, from (3.11) and integration by parts, we also have

$$(3.13) \quad r_s(v) = r_{s,K}(v) = (\nabla \cdot \boldsymbol{\sigma}_s^\Delta, v)_K = -(\boldsymbol{\sigma}_s^\Delta, \nabla v)_K + \sum_{F \in \mathcal{E}_K} \int_F \boldsymbol{\sigma}_s^\Delta \cdot \mathbf{n}_F \llbracket v \rrbracket ds.$$

Given (3.12) with (3.13), it is natural to match and define $\boldsymbol{\sigma}_s^\Delta \in RT(\mathcal{T}_h, s)$ such that

$$(3.14) \quad \int_F \boldsymbol{\sigma}_s^\Delta \cdot \mathbf{n}_F \phi ds = \begin{cases} \gamma \frac{\alpha_{F, \min}}{h_F} \int_F \llbracket u_k^{dg} \rrbracket \phi ds, & \forall F \in \mathcal{E} \setminus \mathcal{E}_N, \quad \forall \phi \in \mathbb{P}_k(F), \\ 0, & \forall F \in \mathcal{E}_N, \end{cases}$$

and, when, $s \geq 1$,

$$(3.15) \quad (\boldsymbol{\sigma}_s^\Delta, \boldsymbol{\psi})_K = -\delta \sum_{F \in \mathcal{E}_K \setminus \mathcal{E}_N} \int_F \{A \boldsymbol{\psi} \cdot \mathbf{n}_F\}_w^F \llbracket u_k^{dg} \rrbracket ds. \quad \forall \boldsymbol{\psi} \in \mathbb{P}_{s-1}(K)^d.$$

LEMMA 3.1. *The recovered flux $\hat{\boldsymbol{\sigma}}_s^{dg}$ defined in (3.9) where $\boldsymbol{\sigma}_s^\Delta$ is defined in (3.14)-(3.15) belongs to $RT(\mathcal{T}_h, s)$ for any $(0 \leq s \leq k)$. Furthermore, it is locally conservative, satisfying $\hat{\boldsymbol{\sigma}}_s^{dg} \in RT_f(\mathcal{T}_h, s)$.*

Proof. First $\hat{\boldsymbol{\sigma}}_s^{dg} \in RT(\mathcal{T}_h, s)$ is immediate. To prove that $\hat{\boldsymbol{\sigma}}_s^{dg} \in RT_f(\mathcal{T}_h, s)$, by (3.9), integration by parts, the definition of $\boldsymbol{\sigma}_s^\Delta$, (3.12) and (3.10), we have for any $v \in DG(K, s)$:

$$\begin{aligned} &(\nabla \cdot \hat{\boldsymbol{\sigma}}_s^{dg}, v)_K = (\nabla \cdot \tilde{\boldsymbol{\sigma}}_s^{dg}, v)_K + (\nabla \cdot \boldsymbol{\sigma}_s^\Delta, v)_K \\ &= (\nabla \cdot \tilde{\boldsymbol{\sigma}}_s^{dg}, v)_K - (\boldsymbol{\sigma}_s^\Delta, \nabla v)_K + \sum_{F \in \mathcal{E}_K} \langle \boldsymbol{\sigma}_s^\Delta \cdot \mathbf{n}_F, \llbracket v \rrbracket \rangle_F \\ &= (\nabla \cdot \tilde{\boldsymbol{\sigma}}_s^{dg}, v)_K + \sum_{F \in \mathcal{E}_K \setminus \mathcal{E}_N} \delta \int_F \{A \nabla v \cdot \mathbf{n}_F\}_w^F \llbracket u_k^{dg} \rrbracket ds + \sum_{F \in \mathcal{E}_K \setminus \mathcal{E}_N} \gamma \frac{\alpha_{F, \min}}{h_F} \int_F \llbracket u_k^{dg} \rrbracket \llbracket v \rrbracket ds \\ &= (\nabla \cdot \tilde{\boldsymbol{\sigma}}_s^{dg}, v)_K + r_s(v) = (\nabla \cdot \tilde{\boldsymbol{\sigma}}_s^{dg}, v)_K + (f - \nabla \cdot \tilde{\boldsymbol{\sigma}}_s^{dg}, v)_K = (f, v)_K. \end{aligned}$$

This completes the proof of the lemma. \square

The recovered flux here is similar to those introduced in [1, 23] for $s = k$ but with modified weight.

Since $r_s(v)$ in the right-hand side of (3.10) is the residual based on the weighted averaging, we refer to our method as the *Equilibrated Averaging Residual Method (EARM)* to distinguish it from the classical equilibrated residual method introduced in [3].

3.1. Algorithm for the EARM. We now outline the pseudo-algorithm for the EARM. Define

$$RT_f(\mathcal{T}_h, s', s) = \{\boldsymbol{\tau} \in RT(\mathcal{T}_h, s') : \Pi_s(\nabla \cdot \boldsymbol{\tau}) = f_s \text{ in } \Omega \text{ and } \boldsymbol{\tau} \cdot \mathbf{n}_F = g_{s,F} \text{ on } F \in \mathcal{E}_N\}.$$

Here, Π_s denotes the L^2 -orthogonal projection onto the space $DG(\mathcal{T}_h, s)$. We summarize the seudo-algorithm of EARM in [Algorithm 3.1](#).

Algorithm 3.1 The pseudocode for EARM

- 1: **Input:** Finite element solution $u_h \in DG(\mathcal{T}_h, k)$.
- 2: Step 1: Compute the weighted averaging flux by [\(3.6\)](#)–[\(3.7\)](#):

$$\tilde{\boldsymbol{\sigma}}_{k-1}(u_h) \in RT(\mathcal{T}_h, k-1) \quad \text{or} \quad \tilde{\boldsymbol{\sigma}}_s(u_h), \quad 0 \leq s \leq k-1.$$

- 3: Step 2: Solve for a correction flux: $\boldsymbol{\sigma}_s^\Delta \in RT(\mathcal{T}_h, s)$ such that

$$(3.16) \quad (\nabla \cdot \boldsymbol{\sigma}_s^\Delta, v)_K = r_s(v) \quad \forall v \in DG(\mathcal{T}_h, s),$$

where $r_s(v) = (f - \nabla \cdot \tilde{\boldsymbol{\sigma}}_s(u_h), v)_K$.

- 4: Step 3: Obtain the equilibrated flux:

$$\hat{\boldsymbol{\sigma}}_h = \tilde{\boldsymbol{\sigma}}_{k-1}(u_h) + \boldsymbol{\sigma}_s^\Delta \in RT_f(\mathcal{T}_h, \max(s, k-1), s),$$

or

$$\hat{\boldsymbol{\sigma}}_h = \tilde{\boldsymbol{\sigma}}_s(u_h) + \boldsymbol{\sigma}_s^\Delta \in RT_f(\mathcal{T}_h, s, s).$$

4. ON-EARM for Conforming FEM. Define the k -th order ($k \geq 1$) conforming finite element spaces by

$$CG(\mathcal{T}_h, k) = \{v \in H^1(\Omega) : v|_K \in \mathbb{P}_k(K), \quad \forall K \in \mathcal{T}_h\}$$

and

$$CG_{0,\Gamma_D}(\mathcal{T}_h, k) = H_{0,\Gamma_D}^1(\Omega) \cap CG(\mathcal{T}_h, k).$$

The conforming finite element solution of order k is to find $u_k^{cg} \in CG_{0,\Gamma_D}(\mathcal{T}_h, k)$ such that

$$(4.1) \quad (A \nabla u_k^{cg}, \nabla v)_\Omega = (f, v)_\Omega - \langle g, v \rangle_{\Gamma_N}, \quad \forall v \in CG_{0,\Gamma_D}(\mathcal{T}_h, k).$$

To compute the correction flux in [\(3.16\)](#) for u_k^{cg} , a more careful treatment is required than in the DG case. As in the conforming setting, a locally conservative flux does not admit a straightforward closed-form expression.

We start by first checking the compatibility of the variational problem. Note that for any $v \in CG_{0,\Gamma_D}(\mathcal{T}_h, k-1)$, by the definition of $\tilde{\boldsymbol{\sigma}}_{k-1}^{cg} := \tilde{\boldsymbol{\sigma}}_{k-1}(u_k^{cg})$ and integration by parts, there holds

$$(4.2) \quad r(v) := (f, v) - (\nabla \cdot \tilde{\boldsymbol{\sigma}}_{k-1}^{cg}, v) = (f, v) - (A \nabla u_k^{cg}, \nabla v) - \langle g, v \rangle_{\Gamma_N} = 0.$$

Specifically, for any $v \in CG_{0,\Gamma_D}(\mathcal{T}_h, s)$, $s \leq k-1$, and $\text{supp}(v) = K$ for any $K \in \mathcal{T}_h$, we also have $r(v) = 0$. The residual problem [\(3.16\)](#) then should satisfy

$$(4.3) \quad 0 = r(v) = (\nabla \cdot \boldsymbol{\sigma}_s^\Delta, v)_K = -(\boldsymbol{\sigma}_s^\Delta, \nabla v)_K = 0.$$

To ensure the compatibility in (4.3), it is natural to impose the following restriction for the interior degree of freedom of $\boldsymbol{\sigma}_s^\Delta$ by

$$(4.4) \quad (\boldsymbol{\sigma}_s^\Delta, \boldsymbol{\psi})_K = 0 \quad \forall \boldsymbol{\psi} \in \mathbb{P}_{s-1}(K)^d \quad \text{when } s \geq 1.$$

Define the space for $s \geq 1$,

$$\mathring{RT}(\mathcal{T}_h, s) = \{ \boldsymbol{\tau} \in RT(\mathcal{T}_h, s) : (\boldsymbol{\tau}, \boldsymbol{\psi})_K = 0 \ \forall \boldsymbol{\psi} \in \mathbb{P}_{s-1}(K)^d, K \in \mathcal{T}_h, \boldsymbol{\tau} \cdot \mathbf{n}_F = 0, F \in \mathcal{E}_N \}.$$

In the case $s = 0$, we let $\mathring{RT}(\mathcal{T}_h, 0) = RT(\mathcal{T}_h, 0)$. Then, (3.16), becomes finding $\boldsymbol{\sigma}_s^\Delta \in \mathring{RT}(\mathcal{T}_h, s)$ such that

$$(4.5) \quad \sum_{F \in \mathcal{E} \setminus \mathcal{E}_N} \int_F \boldsymbol{\sigma}_s^\Delta \cdot \mathbf{n}_F [v] ds = r(v) \quad \forall v \in DG(\mathcal{T}_h, s).$$

We have the following compatibility result for (4.5).

LEMMA 4.1. *Let $\mathcal{A}(\boldsymbol{\tau}_h, v) := \sum_{F \in \mathcal{E} \setminus \mathcal{E}_N} \langle \boldsymbol{\tau}_h \cdot \mathbf{n}_F, [v] \rangle_F$ be a bilinear form defined on $\boldsymbol{\tau}_h \in \mathring{RT}(\mathcal{T}_h, s) \times DG(\mathcal{T}_h, s)$, $0 \leq s \leq k-1$. There holds*

$$(4.6) \quad \mathcal{A}(\boldsymbol{\tau}_h, v) = r(v) = 0, \quad \forall v \in CG_{0,\Gamma_D}(\mathcal{T}_h, s).$$

where $r(v) = (f - \nabla \cdot \tilde{\boldsymbol{\sigma}}_{k-1}^{cg}, v)_\Omega$.

Proof. The proof is immediate. \square

4.1. Null-Space Elimination for $\boldsymbol{\sigma}_s^\Delta$. Note that (4.5) has infinitely many solutions given the kernel of divergence-free space. In this subsection, we derive a recovery method that removes the null-space and restricts the correction flux in the orthogonal complement of divergence-free null-space.

Denote the divergence-free space in $\mathring{RT}(\mathcal{T}_h, s)$ as

$$\mathring{RT}^0(\mathcal{T}_h, s) = \{ \boldsymbol{\tau} \in \mathring{RT}(\mathcal{T}_h, s) : \nabla \cdot \boldsymbol{\tau} = 0 \}.$$

Also denote by $\mathring{RT}^0(\mathcal{T}_h, s)^\perp$ the orthogonal complement of the divergence free space $\mathring{RT}^0(\mathcal{T}_h, s)$.

Now for any $w \in DG(\mathcal{T}_h, s)$, define a mapping $\mathbf{S} : w \in DG(\mathcal{T}_h, s) \rightarrow \mathbf{S}(w) \in \mathring{RT}(\mathcal{T}_h, s)$ such that

$$(4.7) \quad \mathbf{S}(w) \cdot \mathbf{n}_F|_F = A_F h_F^{-1} [w]|_F \quad \forall F \in \mathcal{E} \setminus \mathcal{E}_N,$$

where $A_F = \min(\alpha_F^+, \alpha_F^-)$ when $F \in \mathcal{E}_I$ and $A_F = \alpha_F^-$ when $F \in \mathcal{E}_D$.

LEMMA 4.2. *The following relationship holds:*

$$\{ \mathbf{S}(w) : w \in DG(\mathcal{T}_h, s) \} \subset \mathring{RT}^0(\mathcal{T}_h, s)^\perp.$$

Proof. We first observe that for any $\boldsymbol{\tau}_h \in \mathring{RT}^0(\mathcal{T}_h, s)$, there holds

$$(4.8) \quad 0 = (\nabla \cdot \boldsymbol{\tau}_h, v)_{\mathcal{T}_h} \Leftrightarrow \sum_{F \in \mathcal{E} \setminus \mathcal{E}_N} \langle \boldsymbol{\tau}_h \cdot \mathbf{n}_F, [v] \rangle_F = \mathcal{A}(\boldsymbol{\tau}_h, v) = 0 \quad \forall v \in DG(\mathcal{T}_h, s).$$

Thus, $\boldsymbol{\tau}_h \in \mathring{RT}^0(\mathcal{T}_h, s)^\perp$ if and only if

$$(4.9) \quad \mathcal{A}(\boldsymbol{\tau}_h, v) = 0 \quad \forall v \in DG(\mathcal{T}_h, s) \Rightarrow \boldsymbol{\tau}_h \equiv 0.$$

Therefore, to prove that $\mathbf{S}(w) \in \mathring{RT}^0(\mathcal{T}_h, s)^\perp$, it is sufficient to prove that $\mathbf{S}(w)$ satisfies (4.9) for all $w \in DG(\mathcal{T}_h, s)$. Assuming

$$(4.10) \quad \mathcal{A}(\mathbf{S}(w), v) = 0 \quad \forall v \in DG(\mathcal{T}_h, s),$$

immediately yields

$$(4.11) \quad \mathcal{A}(\mathbf{S}(w), w) = 0,$$

i.e., $\|A_F^{1/2}h_F^{-1}\llbracket w \rrbracket\|_{\mathcal{E} \setminus \mathcal{E}_N} = 0$, hence, $\|\mathbf{S}(w) \cdot \mathbf{n}_F\|_{\mathcal{E} \setminus \mathcal{E}_N} \equiv 0$. This completes the proof of the lemma. \square

Thanks to [Lemma 4.2](#), we reformulate the problem (4.5) by restricting the flux in the space of $\mathring{RT}^0(\mathcal{T}_h, s)^\perp$ as following: finding $u_s^\Delta \in DG(\mathcal{T}_h, s)$ such that

$$(4.12) \quad \mathcal{A}(\llbracket u_s^\Delta \rrbracket, \llbracket v \rrbracket) = r(v) \quad \forall v \in DG(\mathcal{T}_h, s),$$

where

$$\mathcal{A}(\llbracket u_s^\Delta \rrbracket, \llbracket v \rrbracket) := \sum_{F \in \mathcal{E} \setminus \mathcal{E}_N} \int_F A_F h_F^{-1} \llbracket u_s^\Delta \rrbracket \llbracket v \rrbracket ds.$$

Note that only the information of $\llbracket u_s^\Delta \rrbracket$ on facets $\mathcal{E} \setminus \mathcal{E}_N$ is used in the formulation. We further define for any $s \geq 1$ the quotient spaces:

$$DG^0(\mathcal{T}_h, s) = \{v \in DG(\mathcal{T}_h, s) : v|F = 0 \forall F \in \mathcal{E}_N\} / \{v \in CG(\mathcal{T}_h, s)\}.$$

Here we have used A/B to denote the quotient space of A by B . (4.12) is then equivalent to finding $u_s^\Delta \in DG^0(\mathcal{T}_h, s)$ such that

$$(4.13) \quad \mathcal{A}(\llbracket u_s^\Delta \rrbracket, \llbracket v \rrbracket)_F = r(v) \quad \forall v \in DG^0(\mathcal{T}_h, s).$$

One feature of (4.13) is the well-posedness thanks to the same trial and test spaces along with continuity and coercivity in the space of $DG^0(\mathcal{T}_h, s)$.

LEMMA 4.3. (4.13) has a unique solution $u_s^\Delta \in DG^0(\mathcal{T}_h, s)$ for all integers $0 \leq s \leq k-1$.

Proof. We first have that the bilinear form $\mathcal{A}(\llbracket u_s^\Delta \rrbracket, \llbracket v \rrbracket)_F$ is continuous and coercive in the space of $DG^0(\mathcal{T}_h, s)$ under the norm:

$$(4.14) \quad \llbracket v \rrbracket = \sqrt{\sum_{F \in \mathcal{E} \setminus \mathcal{E}_N} h_F^{-1} \|A_F^{1/2} \llbracket v \rrbracket\|_F^2}.$$

Then, by the Lax-Milgram theorem, (4.13) has a unique solution for all $0 \leq s \leq k-1$. \square

Remark 4.4. When $s = 0$, our method coincides with the equilibrated flux recovered in [\[29\]](#). Though the solution of (4.13) is unique, it renders a global problem. However, the number of degrees of freedom for the global problem is much less than the original problem, as it includes only unknowns restricted to facet degrees of freedom.

Moreover, in two dimensions, for $1 \leq s \leq k-1$, we can localize it using the same techniques as in [6] by replacing the exact integrals, $\int_F A_F h_F^{-1} \llbracket u_s^\Delta \rrbracket \llbracket v \rrbracket ds$, with an inexact Gauss-Lobatto quadrature. With Gauss-Lobatto quadrature in two dimensions, our recovered flux coincides with that in [6]. Furthermore, the recovered flux can be computed entirely explicitly, as shown in [18].

LEMMA 4.5. *Define for some $0 \leq s \leq k-1$*

$$(4.15) \quad \hat{\boldsymbol{\sigma}}_h^{cg} = \tilde{\boldsymbol{\sigma}}_{k-1}^{cg} + \boldsymbol{\sigma}_s^\Delta,$$

where $\boldsymbol{\sigma}_s^\Delta = \mathbf{S}(u_s^\Delta)$ in which u_s^Δ is the solution to (4.13). Then $\hat{\boldsymbol{\sigma}}_h^{cg} \in RT(\mathcal{T}_h, k-1, s)$ satisfies

$$(4.16) \quad (\nabla \cdot \hat{\boldsymbol{\sigma}}_h^{cg}, v) = (f, v) \quad \forall v \in DG(\mathcal{T}_h, s).$$

Proof. It is sufficient to prove (4.16) for any $v \in \mathbb{P}_s(K) \subset DG(\mathcal{T}_h, s)$. By the definitions, integration by parts, (4.13)

$$(4.17) \quad \begin{aligned} (\nabla \cdot \hat{\boldsymbol{\sigma}}_h^{cg}, v)_K &= (\nabla \cdot \tilde{\boldsymbol{\sigma}}_{k-1}^{cg}, v)_K + (\nabla \cdot \boldsymbol{\sigma}_s^\Delta, v)_K \\ &= (\nabla \cdot \tilde{\boldsymbol{\sigma}}_{k-1}^{cg}, v)_K + (\boldsymbol{\sigma}_s^\Delta, \nabla v)_K + (\boldsymbol{\sigma}_s^\Delta \cdot \mathbf{n}_F, \llbracket v \rrbracket)_{\partial K} \\ &= (\nabla \cdot \tilde{\boldsymbol{\sigma}}_{k-1}^{cg}, v)_K + \sum_{F \in \mathcal{E}_K \setminus \mathcal{E}_N} (A_F h_F^{-1} \llbracket u_s^\Delta \rrbracket, \llbracket v \rrbracket)_F = (\nabla \cdot \tilde{\boldsymbol{\sigma}}_{k-1}^{cg}, v)_K + r(v) \\ &= (\nabla \cdot \tilde{\boldsymbol{\sigma}}_{k-1}^{cg}, v)_K + (f, v)_K - (\nabla \cdot \tilde{\boldsymbol{\sigma}}_{k-1}^{cg}, v)_K = (f, v)_K. \end{aligned}$$

We have completed the proof of the lemma. \square

LEMMA 4.6. *Define for some $0 \leq s \leq k-1$*

$$(4.18) \quad \hat{\boldsymbol{\sigma}}_s^{cg} = \tilde{\boldsymbol{\sigma}}_s^{cg} + \boldsymbol{\sigma}_s^\Delta,$$

where $\boldsymbol{\sigma}_s^\Delta = \mathbf{S}(u_s^\Delta)$ in which u_s^Δ is the solution to (4.13). Then $\hat{\boldsymbol{\sigma}}_s^{cg} \in RT_f(\mathcal{T}_h, s)$ satisfies

$$(4.19) \quad (\nabla \cdot \hat{\boldsymbol{\sigma}}_s^{cg}, v) = (f, v) \quad \forall v \in DG(\mathcal{T}_h, s).$$

Proof. (4.19) can be proved similarly as in Lemma 4.5 and the fact that

$$(\nabla \cdot \tilde{\boldsymbol{\sigma}}_s^{cg}, v)_K = (\nabla \cdot \tilde{\boldsymbol{\sigma}}_{k-1}^{cg}, v)_K \quad \forall v \in DG(\mathcal{T}_h, s). \quad \square$$

5. Automatic Global Reliability. We first cite the following reliability result proved in [16].

THEOREM 5.1. *Let $u \in H_D^1(\Omega)$ be the solution of (2.1). In two and three dimensions, for all $w \in H^1(\mathcal{T}_h)$, we have*

$$\|A^{1/2} \nabla_h(u - w)\|^2 = \inf_{\boldsymbol{\tau} \in \Sigma_f(\Omega)} \|A^{-1/2} \boldsymbol{\tau} + A^{1/2} \nabla_h w\|^2 + \inf_{v \in H_D^1(\Omega)} \|A^{1/2} \nabla_h(v - w)\|^2.$$

where

$$\Sigma_f(\Omega) = \left\{ \boldsymbol{\tau} \in H(\text{div}; \Omega) : \nabla \cdot \boldsymbol{\tau} = f \text{ in } \Omega \text{ and } \boldsymbol{\tau} \cdot \mathbf{n} = g \text{ on } \Gamma_N \right\}.$$

Based on the theorem and Corollary 3.5 in [16], the construction of an equilibrated a posteriori error estimator for discontinuous finite element solutions is reduced to

recover an equilibrated in $\Sigma_f(\Omega)$ and to recover either a potential function in $H^1(\Omega)$ or a curl free vector-valued function in $H(\text{curl}; \Omega)$. In this paper, we focus on the part of equilibrated flux recovery. We note that $\inf_{\boldsymbol{\tau} \in \Sigma_f(\Omega)} \|A^{-1/2}\boldsymbol{\tau} + A^{1/2}\nabla_h w\|^2$ is usually referred to as the conforming error of w .

Note that in our case, the recovered flux lies in $RT_f(\mathcal{T}_h, s)$ or $RT_f(\mathcal{T}_h, k-1, s)$, which is not generally in $\Sigma_f(\Omega)$. We can adjust and obtain the following reliability result similar to [Theorem 5.1](#) except with an additional oscillation term on the right,

$$(5.1) \quad \begin{aligned} \|A^{1/2}\nabla_h(u - u_k^{cg})\|^2 &\leq \|A^{-1/2}\hat{\boldsymbol{\sigma}}_h + A^{1/2}\nabla_h u_k^{cg}\|^2 \\ &+ \inf_{v \in H_D^1(\Omega)} \|A^{1/2}\nabla_h(v - u_k^{cg})\|^2 + c\|f - f_s\|_{\Omega}^2. \end{aligned}$$

This additional oscillation term is of higher order when $f|_K$ is smooth for all $K \in \mathcal{T}_h$. It is usually neglected in the computation.

We define the local indicator for the conforming error by

$$(5.2) \quad \eta_{\sigma, K} = \|A^{-1/2}(\hat{\boldsymbol{\sigma}}_h - \boldsymbol{\sigma}_h)\|_K$$

where $\boldsymbol{\sigma}_h = -A\nabla u_h$ is the numerical flux corresponding to the finite element solution u_h and $\hat{\boldsymbol{\sigma}}_h$ is a recovered equilibrated flux based on $\boldsymbol{\sigma}_h$. The global estimator is then defined as

$$(5.3) \quad \eta_{\sigma} = \left(\sum_{K \in \mathcal{T}_h} \eta_{\sigma, K}^2 \right)^{1/2} = \|A^{-1/2}(\hat{\boldsymbol{\sigma}}_h - \boldsymbol{\sigma}_h)\|_{0, \Omega},$$

in which $\hat{\boldsymbol{\sigma}}_h$ is the recovered equilibrated flux based on u_h .

6. Robust Efficiency. In this section, we prove robust efficiency of the error indicator defined in (5.2) for the recovered flux $\hat{\boldsymbol{\sigma}}_h = \hat{\boldsymbol{\sigma}}_h^{cg}$ from [Lemma 4.5](#), when applied to the conforming finite element solution u_k^{cg} . The remaining cases for $\hat{\boldsymbol{\sigma}}_s^{cg}, 0 \leq s \leq k-1$ can be treated similarly. Here, *robustness* means that the efficiency constant is independent of the jump in the diffusion coefficient $A(x)$.

For recovered fluxes constructed from discontinuous Galerkin solutions, we refer to [\[1, 23, 16, 3\]](#).

For simplicity, we assume that the diffusion coefficient $A(x)$ is a piecewise constant function and that $A_F^- \leq A_F^+$ for all $F \in \mathcal{E}_I$. From here to thereafter, we use $a \lesssim b$ to denote that $a \leq Cb$ for a generic constant that is independent of the mesh size and the jump of A .

For simplicity, we restrict our analysis in the two dimensions. To show that the efficiency constant for the conforming case is independent of the jump of $A(x)$, as usual, we assume that the distribution of the coefficients A_K for all $K \in \mathcal{T}_h$ is locally quasi-monotone [\[30\]](#), which is slightly weaker than Hypothesis 2.7 in [\[7\]](#). The assumption has been used in the literature and remains essential for rigorous theoretical proofs. However, numerical experiments and practical applications indicate that this assumption is not necessary in computations, as the method performs reliably even when it does not strictly hold, e.g., see [\[14\]](#).

For convenience of readers, we restate the definition of quasi-monotonicity. Let ω_z be the union of all elements having z as a vertex. For any $z \in \mathcal{N}$, let

$$\hat{\omega}_z = \{K \in \omega_z : A_K = \max_{K' \in \omega_z} A_{K'}\}.$$

DEFINITION 6.1. *Given a vertex $z \in \mathcal{N}$, the distribution of the coefficients A_K , $K \in \omega_z$, is said to be quasi-monotone with respect to the vertex z if there exists a subset $\tilde{\omega}_{K,z,qm}$ of ω_z such that the union of elements in $\tilde{\omega}_{K,z,qm}$ is a Lipschitz domain and that*

- if $z \in \mathcal{N} \setminus \mathcal{N}_D$, then $\{K\} \cup \hat{\omega}_z \subset \tilde{\omega}_{K,z,qm}$ and $A_K \leq A_{K'} \forall K' \in \tilde{\omega}_{K,z,qm}$;
- if $z \in \mathcal{N}_D$, then $K \in \tilde{\omega}_{K,z,qm}$, $\partial \tilde{\omega}_{K,z,qm} \cap \Gamma_D \neq \emptyset$, and $A_K \leq A_{K'} \forall K' \in \tilde{\omega}_{K,z,qm}$.

The distribution of the coefficients A_K , $K \in \mathcal{T}$, is said to be locally quasi-monotone if it is quasi-monotone with respect to every vertex $z \in \mathcal{N}$.

For a function $v \in DG(\mathcal{T}_h, s)$, we choose to employ the classical Lagrangian basis functions. For a function $v \in DG^0(\mathcal{T}_h, s)$, since only $\llbracket v \rrbracket|_{\mathcal{E} \setminus \mathcal{E}_N}$ is needed, from here to thereafter, we assume that v satisfies the following conditions.

1. The interior degrees of freedom of v are zero, i.e., $v(\mathbf{x}_{i,K}) = 0, i = 1, \dots, m_s$.
2. Let $\{\mathbf{x}_{i,F}\}_{i=1}^{s-1}$ ($s \geq 1$) be the set of all Lagrange points on F excluding the vertices $\mathbf{x}_{s,F}$ and $\mathbf{x}_{e,F}$ for the space $P_k(F)$. For each $F \in \mathcal{E}_I$ and $\mathbf{x}_{i,F} \in F$, let $v|_{K_F^+}(\mathbf{x}_{i,F}) = 0$.
3. For each $z \in \mathcal{N}$, we denote by K_z be a element in $\hat{\omega}_z$ and let $v|_{K_z}(z) = 0$.
4. When $F \in \mathcal{E}_N$, we simply let $v|_F \equiv 0$.

It's not difficult to prove that with the above four types of restrictions, any function $v \in DG^0(\mathcal{T}_h, s)$ is uniquely determined.

LEMMA 6.2 (Uniqueness in $DG^0(\mathcal{T}_h, s)$). *Let $u, v \in DG^0(\mathcal{T}_h, s)$ satisfy the above assumptions. If*

$$\llbracket u \rrbracket = \llbracket v \rrbracket \quad \text{on } \mathcal{E} \setminus \mathcal{E}_N,$$

then

$$u \equiv v \quad \text{in } \Omega.$$

Proof. Let $w := u - v \in DG^0(\mathcal{T}_h, s)$. By the assumption $\llbracket u \rrbracket = \llbracket v \rrbracket$ on $\mathcal{E} \setminus \mathcal{E}_N$ and $u|_F = v|_F \equiv 0$ for $F \in \mathcal{E}_N$, we have

$$\llbracket w \rrbracket = 0 \quad \text{on } \mathcal{E}.$$

Hence, $w \in CG(\mathcal{T}_h, s)$ and $w = 0$ on $\partial\Omega$.

Moreover, by Assumption 1, w vanishes at all interior degrees of freedom. By Assumption 2, w vanishes at all interior facet Lagrange points, except possibly at the vertices. Finally, by Assumption 3, w vanishes at all vertex degrees of freedom. Hence, all degrees of freedom of w are zero, and therefore

$$w \equiv 0.$$

□

Consequently, $u \equiv v$. This completes the proof of the lemma.

We first prove the following lemma.

LEMMA 6.3. *For any $v \in DG^0(\mathcal{T}_h, s)$, there holds*

$$(6.1) \quad \|A^{1/2} \nabla v\|_{\mathcal{T}_h} \leq C \sum_{F \in \mathcal{E} \setminus \mathcal{E}_N} h_F^{-1/2} A_F^{1/2} \|\llbracket v \rrbracket\|_F.$$

where the constant C is independent of the mesh and the jump of the coefficient $A(x)$,

Proof. For any $K \in \mathcal{T}_h$, we first have that

$$(6.2) \quad \|\nabla v\|_K \lesssim \sum_{z \in \mathcal{N}_K} |v_K(z)| + \sum_{F \in \mathcal{E}_K} \sum_{i=1}^{s-1} |v_K(\mathbf{x}_{i,F})|.$$

Fix any $z \in \mathcal{N}_K$. If $K = K_z$, we have $v_K(z) = 0$. If $K \neq K_z$, applying the triangle equality and the property of v yields

$$(6.3) \quad |v_K(z)| \leq \sum_{F \subset \tilde{\omega}_{K,z,qm} \cap \mathcal{E}_z} |\llbracket v \rrbracket|_F(z).$$

Here we choose $\tilde{\omega}_{K,z,qm}$ to be open, so $\tilde{\omega}_{K,z,qm} \cap \mathcal{E}_z$ does not contain the two boundary edges $\partial_{\tilde{\omega}_{K,z,qm}} \cap \mathcal{E}_z$. Since $A(x)$ is monotone along $\tilde{\omega}_{K,z,qm}$, we have

$$(6.4) \quad A_K^{1/2} |v_K(z)| \leq \sum_{F \subset \tilde{\omega}_{K,z,qm} \cap \mathcal{E}_z} A_F^{1/2} |\llbracket v \rrbracket|_F(z).$$

Finally, for any $\mathbf{x}_{i,F}$, $i = 1, \dots, s-1$ and $F \in \mathcal{E}_K$ we have

$$(6.5) \quad A_K^{1/2} |v_K(\mathbf{x}_{i,F})| = \begin{cases} 0 & \text{if } K = K_F^+ \\ A_K^{1/2} |\llbracket v \rrbracket|_F(\mathbf{x}_{i,F}) & \text{if } K = K_F^- \end{cases} \leq A_F^{1/2} |\llbracket v \rrbracket|_F(\mathbf{x}_{i,F}).$$

Recall we assumed that $A_F^- \leq A_F^+$. Combing (6.2)–(6.5), we have for any $K \in \mathcal{T}_h$,

$$(6.6) \quad \begin{aligned} \|A^{1/2} \nabla v\|_K &\lesssim \sum_{z \in \mathcal{N}_K} \sum_{F \in \mathcal{E}_z} A_F^{1/2} |\llbracket v \rrbracket|_F(z) + \sum_{F \in \mathcal{E}_K} \sum_{i=1}^{s-1} A_F^{1/2} |\llbracket v \rrbracket|_F(\mathbf{x}_{i,F}) \\ &\lesssim \sum_{z \in \mathcal{N}_K} \sum_{F \in \mathcal{E}_z} A_F^{1/2} h_F^{-1/2} \|\llbracket v \rrbracket\|_F. \end{aligned}$$

and, hence, (6.1). This completes the proof of the lemma. \square

LEMMA 6.4. *Let $u_s^\Delta \in DG^0(\mathcal{T}_h, s)$ be the solution of (4.13). We have the following estimation for $\|u_s^\Delta\|$:*

$$(6.7) \quad \|u_s^\Delta\| \leq C \|A^{1/2} \nabla(u - u_k^{cg})\| + \text{osc}(f),$$

where the constant C is independent of the mesh size and the jump of the coefficient of $A(x)$.

Proof. First, we observe that

$$(6.8) \quad \|u_s^\Delta\| = \sup_{v \in DG^0(\mathcal{T}_h, s), \|v\|=1} \mathcal{A}(u_s^\Delta, v) = \sup_{v \in DG^0(\mathcal{T}_h, s), \|v\|=1} r(v).$$

Applying integration by parts, the definition of $\tilde{\sigma}_{k-1}^{cg}$ and (3.2), we have

$$\begin{aligned} r(v) &= (f - \nabla \cdot \tilde{\sigma}_{k-1}^{cg}, v)_\Omega = (f, v)_\Omega + \sum_{K \in \mathcal{T}_h} ((\tilde{\sigma}_{k-1}^{cg}, \nabla v)_K - \langle \tilde{\sigma}_{k-1}^{cg} \cdot \mathbf{n}_K, v \rangle_{\partial K}) \\ &= (f, v)_\Omega - \sum_{K \in \mathcal{T}_h} (A \nabla u_k^{cg}, \nabla v)_K + \sum_{F \in \mathcal{E} \setminus \mathcal{E}_N} \langle \{A \nabla u_k^{cg} \cdot \mathbf{n}_F\}_w^F, \llbracket v \rrbracket \rangle_F \\ &= (f + \nabla \cdot A \nabla u_k^{cg}, v)_\Omega - \sum_{F \in \mathcal{E}_I} \langle (\llbracket A \nabla u_k^{cg} \cdot \mathbf{n}_F \rrbracket, \{v\}_F^w) \rangle_F \end{aligned}$$

By the triangle and Cauchy Schwartz inequalities, and (3.1), we have for any $F \in \mathcal{E}_I$,

$$(6.9) \quad \begin{aligned} &\langle (\llbracket A \nabla u_k^{cg} \cdot \mathbf{n}_F \rrbracket, \{v\}_F^w) \rangle_F \lesssim \| \llbracket A \nabla u_k^{cg} \cdot \mathbf{n}_F \rrbracket \|_F (\omega_F^+ \|v_{K_F^-}\|_F + \omega_F^- \|v_{K_F^+}\|_F) \\ &\lesssim \|A_{F,max}^{-1/2} \llbracket A \nabla u_k^{cg} \cdot \mathbf{n}_F \rrbracket\|_F (\|(A^{1/2} v)_{K_F^-}\|_F + \|(A^{1/2} v)_{K_F^+}\|_F). \end{aligned}$$

Applying similar techniques as in the proof of [Lemma 6.3](#) we can have the following bounds

$$(6.10) \quad (\|(A^{1/2}v)_{K_F^-}\|_F + \|(A^{1/2}v)_{K_F^+}\|_F) \lesssim \sum_{z \in \mathcal{N}_F} \sum_{F \in \mathcal{E}_z} A_F^{1/2} \|\llbracket v \rrbracket\|_F,$$

and

$$(6.11) \quad \|A^{1/2}v\|_K \lesssim \sum_{z \in \mathcal{N}_K} \sum_{F \in \mathcal{E}_z} A_F^{1/2} h_F^{1/2} \|\llbracket v \rrbracket\|_F$$

Finally, applying (6.8)–(6.11) and the Cauchy Schwartz inequality, and the fact that $\|v\| = 1$, we have

$$\begin{aligned} r(v) &\leq \sqrt{\sum_{K \in \mathcal{T}_h} h_K^2 \|A^{-1/2}(f + \nabla \cdot A \nabla u_k^{cg})\|_K^2} \sqrt{\sum_{K \in \mathcal{T}_h} h_K^{-2} \|A^{1/2}v\|_K^2} \\ &+ \sqrt{\sum_{F \in \mathcal{E} \setminus \mathcal{E}_N} h_F A_{F,max}^{-1} \|\llbracket A \nabla u_k^{cg} \cdot \mathbf{n}_F \rrbracket\|_F^2} \sqrt{\sum_{F \in \mathcal{E} \setminus \mathcal{E}_N} h_F^{-1} (\|A^{1/2}v_{K_F^-}\|_F^2 + \|A^{1/2}v_{K_F^+}\|_F^2)} \\ &\lesssim \sqrt{\sum_{K \in \mathcal{T}_h} h_K^2 \|A^{-1/2}(f + \nabla \cdot A \nabla u_k^{cg})\|_K^2} + \sum_{F \in \mathcal{E} \setminus \mathcal{E}_N} \frac{h_F}{A_{F,max}} \|\llbracket A \nabla u_k^{cg} \cdot \mathbf{n}_F \rrbracket\|_F^2 \|v\|. \end{aligned}$$

From the classical efficiency results, we also have

$$(6.12) \quad h_K \|A^{-1/2}(f + \nabla \cdot A \nabla u_k^{cg})\|_K \lesssim \|A^{1/2} \nabla(u - u_k^{cg})\|_{\omega_K} + \text{osc}(f)$$

and

$$(6.13) \quad \|A_{F,max}^{-1/2} \llbracket A \nabla u_k^{cg} \cdot \mathbf{n}_F \rrbracket\|_F \lesssim \|A^{1/2} \nabla(u - u_k^{cg})\|_{\omega_F} + \text{osc}(f)$$

where ω_K and ω_F are some local neighborhood of K and F , respectively; and the involved constant does not depend on the jump of A . Combining all yields (6.7). This completes the proof of the lemma. \square

THEOREM 6.5. *Recall the local error indicator*

$$(6.14) \quad \eta_{\sigma,K} = \|A^{-1/2} \hat{\sigma}_h^{cg} + A^{1/2} \nabla u_k^{cg}\|_K$$

where $\hat{\sigma}_h^{cg}$ is defined in [Lemma 4.5](#). Then we have the following global efficiency bound:

$$(6.15) \quad \eta_{\sigma} \leq C \|A^{1/2} \nabla(u - u_k^{cg})\|_{\mathcal{T}_h} + \text{osc}(f),$$

where the constant is independent of the mesh and the jump of the coefficient $A(x)$.

Proof. First, applying the triangle inequality,

$$(6.16) \quad \begin{aligned} \eta_{\sigma,K} &= \|A^{-1/2} (\hat{\sigma}_h^{cg} - \tilde{\sigma}_{k-1}^{cg})\|_K + \|A^{-1/2} \tilde{\sigma}_{k-1}^{cg} + A^{1/2} \nabla u_k^{cg}\|_K \\ &= \|A^{-1/2} \sigma_s^{\Delta}\|_K + \|A^{-1/2} \tilde{\sigma}_{k-1}^{cg} + A^{1/2} \nabla u_k^{cg}\|_K. \end{aligned}$$

To bound the second term, we first have by the equivalence of norms, (3.1), (3.8) and (6.13),

$$(6.17) \quad \begin{aligned} \|A^{-1/2} \tilde{\sigma}_{k-1}^{cg} + A^{1/2} \nabla u_k^{cg}\|_K &\lesssim \sum_{F \in \mathcal{E}_K} h_F^{1/2} \|A_K^{-1/2} (\tilde{\sigma}_{k-1}^{cg} + A_K \nabla u_k^{cg}) \cdot \mathbf{n}_F\|_F \\ &\lesssim \sum_{F \in \mathcal{E}_K} h_F^{1/2} \|A_{F,max}^{-1/2} \llbracket A \nabla u_k^{cg} \cdot \mathbf{n}_F \rrbracket\|_F \lesssim \sum_{F \in \mathcal{E}_K} \|A^{1/2} \nabla(u - u_k^{cg})\|_{\omega_F} + \text{osc}(f). \end{aligned}$$

It is then sufficient to prove

$$(6.18) \quad \|A^{-1/2}\boldsymbol{\sigma}_s^\Delta\|_{\mathcal{T}_h} \leq C\|A^{1/2}\nabla(u - u_k^{cg})\|_{\mathcal{T}_h} + \text{osc}(f).$$

By the definition of $\boldsymbol{\sigma}_s^\Delta$, (4.7), we have for each $K \in \mathcal{T}_h$,

$$(6.19) \quad \begin{aligned} \|A^{-1/2}\boldsymbol{\sigma}_s^\Delta\|_K &\lesssim \sum_{F \in \mathcal{E}_K} h_F^{1/2} \|A_K^{-1/2}\boldsymbol{\sigma}_s^\Delta \cdot \mathbf{n}_F\|_F \leq \sum_{F \in \mathcal{E}_K} h_F^{1/2} \|A_K^{-1/2}\mathbf{S}(u_s^\Delta) \cdot \mathbf{n}_F\|_F \\ &\leq \sum_{F \in \mathcal{E}_K} h_F^{-1/2} \|A_K^{-1/2}A_F[u_s^\Delta]\|_F \leq \sum_{F \in \mathcal{E}_K} h_F^{-1/2} \|A_F^{1/2}[u_s^\Delta]\|_F. \end{aligned}$$

This, combining with (6.7), indicates that

$$(6.20) \quad \|A^{-1/2}\boldsymbol{\sigma}_s^\Delta\|_{\mathcal{T}_h} \lesssim \|u_s^\Delta\| \leq C\|A^{1/2}\nabla(u - u_k^{cg})\|_{\mathcal{T}_h} + \text{osc}(f). \quad \square$$

This completes the proof of the Theorem.

7. Numerical Experiments. In this section, we report numerical results for the Kellogg interface problem [12] and the L-shaped benchmark problem in two dimensions, discretized by conforming finite element methods. In three dimensions, we consider a regularized Fichera-corner problem with a vertex singularity. In all cases, we test polynomial degrees $k = 1, 2, 3$, and we set $s = k - 1$ for the recovered flux.

We employ a standard adaptive refinement loop of the form

Solve \rightarrow Estimate \rightarrow Mark \rightarrow Refine \rightarrow .

At each iteration, we compute the conforming finite element solution, evaluate the local error indicators and mark elements for refinement. For marking, we use Dörfler's bulk criterion with parameter $\theta \in (0, 1)$. We sort the elements by η_K^2 in descending order and mark the smallest set \mathcal{M} such that

$$\sum_{K \in \mathcal{M}} \eta_K^2 \geq \theta \sum_{K \in \mathcal{T}_h} \eta_K^2.$$

The marked elements are then refined, and the process is repeated until the stopping criterion is met.

All numerical implementations were carried out in FEniCSx [4], which provides an efficient and reproducible finite element programming framework for assembling variational forms and solving the resulting discrete systems.

EXAMPLE 7.1 (Kellogg's Problem). *Let $\Omega = (-1, 1)^2$ and*

$$u(r, \theta) = r^\beta \mu(\theta)$$

in the polar coordinates at the origin with

$$\mu(\theta) = \begin{cases} \cos((\pi/2 - \sigma)\beta) \cdot \cos((\theta - \pi/2 + \rho)\beta) & \text{if } 0 \leq \theta \leq \pi/2, \\ \cos(\rho\beta) \cdot \cos((\theta - \pi + \sigma)\beta) & \text{if } \pi/2 \leq \theta \leq \pi, \\ \cos(\sigma\beta) \cdot \cos((\theta - \pi - \rho)\beta) & \text{if } \pi \leq \theta \leq 3\pi/2, \\ \cos((\pi/2 - \rho)\beta) \cdot \cos((\theta - 3\pi/2 - \sigma)\beta) & \text{if } 3\pi/2 \leq \theta \leq 2\pi, \end{cases}$$

where σ and ρ are numbers. The function $u(r, \theta)$ satisfies the diffusion equation in (2.1) with $A = \alpha I$, $\Gamma_N = \emptyset$, $f = 0$, and

$$\alpha = \begin{cases} R & \text{in } (0, 1)^2 \cup (-1, 0)^2, \\ 1 & \text{in } \Omega \setminus ([0, 1]^2 \cup [-1, 0]^2). \end{cases}$$

In the test problem, we choose $\beta = 0.1$ which is corresponding to

$$R \approx 161.4476387975881, \quad \rho = \frac{\pi}{4}, \quad \text{and} \quad \sigma \approx -14.92256510455152.$$

Note that the solution $u(r, \theta)$ is only in $H^{1+\beta-\epsilon}(\Omega)$ for some $\epsilon > 0$ and, hence, it is very singular for small β at the origin. This suggests that refinements should be centered mostly around the origin.

For the Kellogg problem, we take $\theta = 0.3$ and stop the adaptive loop once the relative error is below 1%. The final adaptive meshes for $k = 1, 2, 3$ are shown in Figure 1, and the convergence of the true error and the global estimator η is reported in Figure 2. In all cases, the refinement is concentrated near the origin, where the solution is singular. We obtain optimal convergence for each degree. For reference, we include the expected rate $N^{-k/2}$ and the computed convergence rates for the true error. The computed convergence rates for the true error are obtained using `polyfit` in Matlab, which performs a least-squares fit of the error data in a log-log scale to extract the asymptotic slope. For all cases, we observe a consistent computed convergence rate with the optimal convergence rate; the estimator exhibits the same optimal behavior

The average efficiency index takes the values 1.3726, 3.6363, and 6.5877 for $k = 1, 2, 3$, respectively.

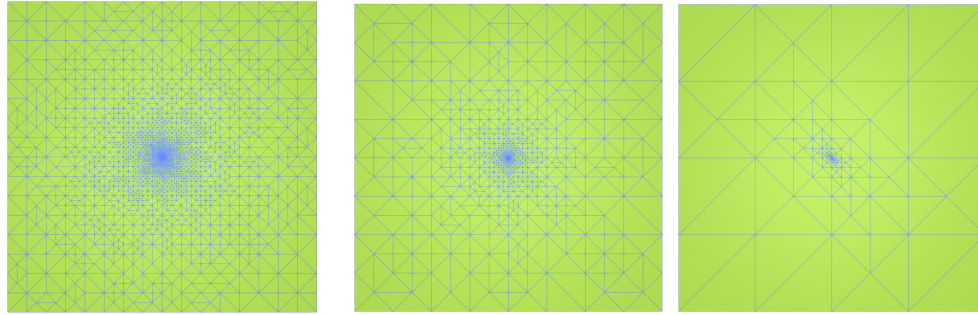


Fig. 1: Example 7.1 Final adaptive meshes for $k = 1, 2, 3$

EXAMPLE 7.2 (L-Shape Problem). *In this example, we test the following problem:*

$$u(r, \theta) = r^{2/3} \sin(2\theta/3), \quad \theta \in [0, 3\pi/2]$$

on the L-shaped domain $\Omega = (-1, 1)^2 \setminus [0, 1] \times [-1, 0]$. Note that this function satisfies (2.1) with $A(x) = I$ and $f = 0$.

For the L-shaped problem, we set $\theta = 0.2$ and use the same stopping criterion as in Example 7.1, i.e., we stop once the relative error falls below 1%. The final adaptive meshes are shown in Figure 3. For all tested degrees, refinement is concentrated near

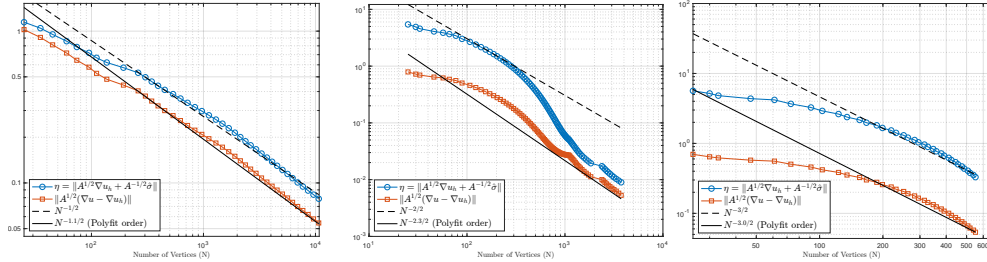


Fig. 2: Example 7.1 Adaptive error convergence results for $k = 1, 2, 3$

the re-entrant corner, where the solution is singular, while the mesh remains coarse elsewhere. The error convergence is reported in Figure 4. In this example, we observe superconvergence: for $k = 2$, the observed orders for both the true error and the estimator are close to 10, and for $k = 3$ the observed orders are around 12.

We emphasize that the estimator remains reliable and closely tracks the true error throughout the adaptive process. The efficiency index takes the values 1.12, 1.79, and 2.25 for $k = 1, 2, 3$, respectively.

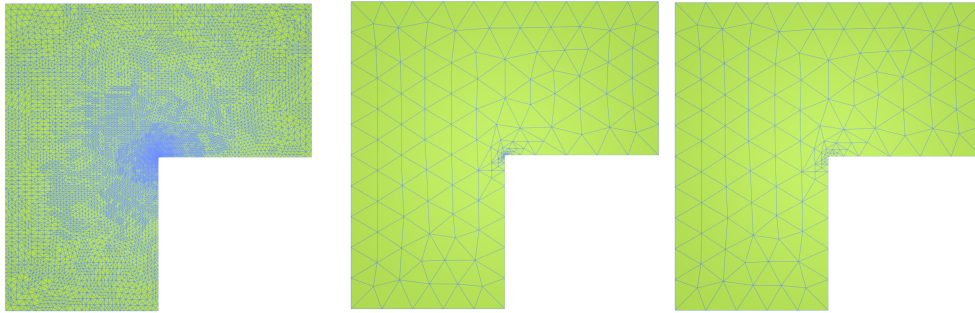


Fig. 3: Example 7.2 Final adaptive meshes for $k = 1, 2, 3$

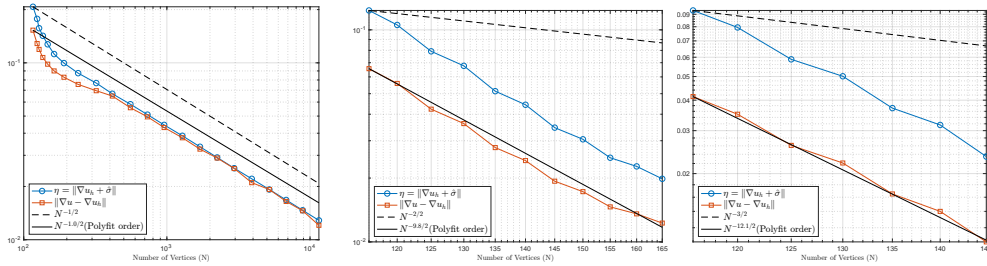


Fig. 4: Example 7.2 Adaptive error convergence results for $k = 1, 2, 3$

EXAMPLE 7.3 (Regularized Fichera corner with vertex singularity). *The Fichera corner problem [27] is the three-dimensional analogue of the two-dimensional L-shaped*

domain. We consider Poisson's equation on

$$\Omega = (-1, 1)^3 \setminus [0, 1]^3,$$

i.e., a cube with one octant removed. To regularize the vertex singularity at the origin, we use the exact solution

$$(7.1) \quad u(x, y, z) = \left(\sqrt{x^2 + y^2 + z^2 + \varepsilon} \right)^q, \quad q = 1/2,$$

where $\varepsilon > 0$ is a small regularization parameter and we choose $\varepsilon = 10^{-6}$.

For the three-dimensional problem, we introduce a small regularization parameter to avoid division-by-zero issues in the right-hand side function f . Specifically, f is defined consistently with the regularized exact solution, as given in (7.1). We choose $\theta = 0.15$ for $k = 1, 3$ and $\theta = 0.3$ for $k = 2$. For $k = 3$, the adaptive loop is terminated when the maximum number of cells reaches 4500, corresponding to a relative error of 1.73%. For $k = 1$, the loop is stopped once the number of cells exceeds 5×10^5 , yielding a relative error of 3.06%. For $k = 2$, the refinement is terminated when the relative error drops below 1%.

The final adaptive meshes are shown in Figure 5. Consistent with the two-dimensional results, refinement is localized near the vertex singularity. The error convergence histories are reported in Figure 6. For $k = 2$ and $k = 3$, we observe slightly more than optimal convergence rates for both the true error and the estimator. For $k = 1$, while the true error exhibits the expected optimal convergence, the estimator converges at a slightly reduced rate, indicating that the efficiency index is not fully uniform across all iterations. The slightly reduced convergence of the estimator may be influenced by numerical effects on very fine meshes (e.g., solver tolerances) around the singularity, once the discretization error becomes comparable to these errors.

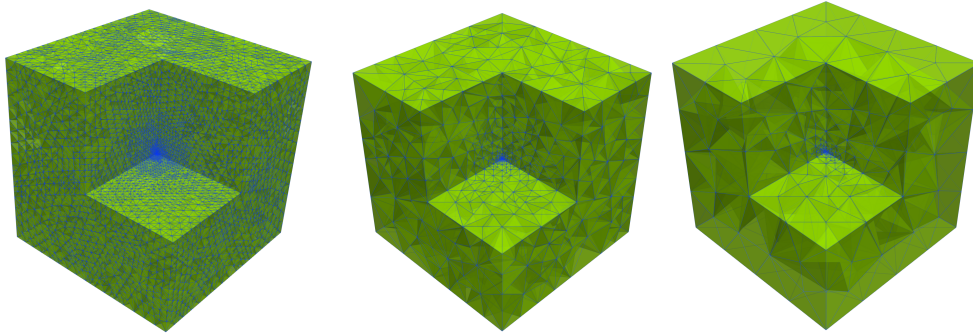


Fig. 5: Example 7.3 Final adaptive meshes for $k = 1, 2, 3$

The efficiency index takes the values 2.93, 5.95, and 6.09 for $k = 1, 2, 3$, respectively.

REFERENCES

[1] M. AINSWORTH, *A posteriori error estimation for discontinuous galerkin finite element approximation*, SIAM Journal on Numerical Analysis, 45 (2007), pp. 1777–1798.

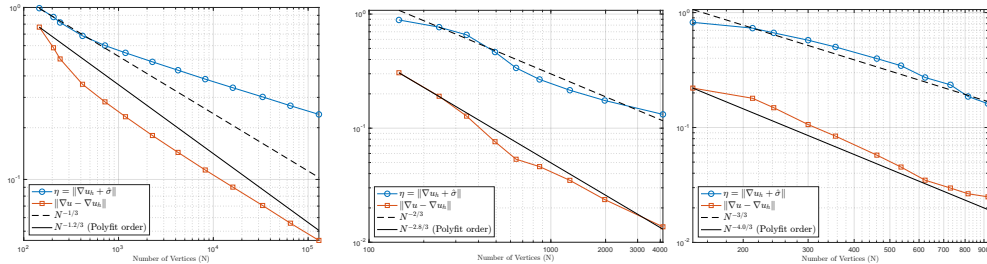


Fig. 6: Example 7.3 Adaptive error convergence results for $k = 1, 2, 3$

- [2] M. AINSWORTH AND J. T. ODEN, *A unified approach to a posteriori error estimation using element residual methods*, Numerische Mathematik, 65 (1993), pp. 23–50.
- [3] M. AINSWORTH AND J. T. ODEN, *A Posteriori Error Estimation in Finite Element Analysis*, vol. 37, John Wiley & Sons, 2000.
- [4] I. A. BARATTA, J. P. DEAN, J. S. DOKKEN, M. HABERA, J. HALE, C. N. RICHARDSON, M. E. ROGNES, M. W. SCROGGS, N. SIME, AND G. N. WELLS, *Dolfinx: the next generation fenics problem solving environment*, (2023).
- [5] P. BASTIAN, *A fully-coupled discontinuous galerkin method for two-phase flow in porous media with discontinuous capillary pressure*, Computational Geosciences, 18 (2014), pp. 779–796.
- [6] R. BECKER, D. CAPATINA, AND R. LUCE, *Local flux reconstructions for standard finite element methods on triangular meshes*, SIAM Journal on Numerical Analysis, 54 (2016), pp. 2684–2706.
- [7] C. BERNARDI AND R. VERFÜRTH, *Adaptive finite element methods for elliptic equations with non-smooth coefficients*, Numerische Mathematik, 85 (2000), pp. 579–608.
- [8] D. BRAESS, *Finite elements: Theory, fast solvers, and applications in solid mechanics*, Cambridge University Press, 2007.
- [9] D. BRAESS, T. FRAUNHOLZ, AND R. H. HOPPE, *An equilibrated a posteriori error estimator for the interior penalty discontinuous galerkin method*, SIAM Journal on Numerical Analysis, 52 (2014), pp. 2121–2136.
- [10] D. BRAESS, V. PILLWEIN, AND J. SCHÖBERL, *Equilibrated residual error estimates are p -robust*, Computer Methods in Applied Mechanics and Engineering, 198 (2009), pp. 1189–1197.
- [11] D. BRAESS AND J. SCHÖBERL, *Equilibrated residual error estimator for edge elements*, Mathematics of Computation, 77 (2008), pp. 651–672.
- [12] R. BRUCE KELLOGG, *On the poisson equation with intersecting interfaces*, Applicable Analysis, 4 (1974), pp. 101–129.
- [13] D. CAI, Z. CAI, AND S. ZHANG, *Robust equilibrated a posteriori error estimator for higher order finite element approximations to diffusion problems*, Numerische Mathematik, 144 (2020), pp. 1–21.
- [14] Z. CAI, C. HE, AND S. ZHANG, *Improved zz a posteriori error estimators for diffusion problems: Conforming linear elements*, Computer Methods in Applied Mechanics and Engineering, 313 (2017), pp. 433–449.
- [15] Z. CAI, C. HE, AND S. ZHANG, *Residual-based a posteriori error estimate for interface problems: nonconforming linear elements*, Mathematics of Computation, 86 (2017), pp. 617–636.
- [16] Z. CAI, C. HE, AND S. ZHANG, *Generalized prager-syng identity and robust equilibrated error estimators for discontinuous elements*, Journal of Computational and Applied Mathematics, (2021), p. 113673.
- [17] Z. CAI AND S. ZHANG, *Robust equilibrated residual error estimator for diffusion problems: Conforming elements*, SIAM Journal on Numerical Analysis, 50 (2012), pp. 151–170.
- [18] D. CAPATINA, A. GOUASMI, AND C. HE, *Robust flux reconstruction and a posteriori error analysis for an elliptic problem with discontinuous coefficients*, Journal of Scientific Computing, 98 (2024), p. 28.
- [19] D. CAPATINA, R. LUCE, H. EL-OTMANY, AND N. BARRAU, *Nitsche's extended finite element method for a fracture model in porous media*, Applicable Analysis, 95 (2016), pp. 2224–2242.
- [20] L. DEMKOWICZ AND M. SWIERCZEK, *An adaptive finite element method for a class of variational inequalities*, in Proceedings of the Italian-Polish Symposium of Continuum Mechanics, Bologna, 1987.

- [21] P. DESTUYNDER AND B. MÉTIVET, *Explicit error bounds in a conforming finite element method*, Mathematics of Computation, 68 (1999), pp. 1379–1396.
- [22] A. ERN, I. MOZOLEVSKI, AND L. SCHUH, *Accurate velocity reconstruction for discontinuous galerkin approximations of two-phase porous media flows*, Comptes Rendus Mathematique, 347 (2009), pp. 551–554.
- [23] A. ERN, S. NICAISE, AND M. VOHRALÍK, *An accurate h (div) flux reconstruction for discontinuous galerkin approximations of elliptic problems*, Comptes Rendus Mathematique, 345 (2007), pp. 709–712.
- [24] A. ERN AND M. VOHRALÍK, *Polynomial-degree-robust a posteriori estimates in a unified setting for conforming, nonconforming, discontinuous galerkin, and mixed discretizations*, SIAM Journal on Numerical Analysis, 53 (2015), pp. 1058–1081.
- [25] P. LADEVEZE AND D. LEGUILLOU, *Error estimate procedure in the finite element method and applications*, SIAM Journal on Numerical Analysis, 20 (1983), pp. 485–509.
- [26] M. G. LARSON AND A. J. NIKLASSON, *A conservative flux for the continuous galerkin method based on discontinuous enrichment*, Calcolo, 41 (2004), pp. 65–76.
- [27] W. F. MITCHELL, *Performance of hp -adaptive strategies for 3d elliptic problems*, (2016).
- [28] J. T. ODEN, L. DEMKOWICZ, W. RACHOWICZ, AND T. A. WESTERMANN, *Toward a universal hp adaptive finite element strategy, part 2: a posteriori error estimation*, Computer methods in applied mechanics and engineering, 77 (1989), pp. 113–180.
- [29] L. H. ODSÆTER, M. F. WHEELER, T. KVAMSDAL, AND M. G. LARSON, *Postprocessing of non-conservative flux for compatibility with transport in heterogeneous media*, Computer Methods in Applied Mechanics and Engineering, 315 (2017), pp. 799–830.
- [30] M. PETZOLDT, *A posteriori error estimators for elliptic equations with discontinuous coefficients*, Advances in Computational Mathematics, 16 (2002), pp. 47–75.
- [31] W. PRAGER AND J. L. SYNGE, *Approximations in elasticity based on the concept of function space*, Quarterly of Applied Mathematics, 5 (1947), pp. 241–269.
- [32] T. VEJCHODSKÝ, *Guaranteed and locally computable a posteriori error estimate*, IMA Journal of Numerical Analysis, 26 (2006), pp. 525–540.
- [33] R. VERFÜRTH, *A note on constant-free a posteriori error estimates*, SIAM journal on numerical analysis, 47 (2009), pp. 3180–3194.
- [34] M. VOHRALÍK AND M. F. WHEELER, *A posteriori error estimates, stopping criteria, and adaptivity for two-phase flows*, Computational Geosciences, 17 (2013), pp. 789–812.